DE GRUYTER

Autex Research Journal, Vol. 24, No. 1, 2024, 20230022, DOI 10.1515/aut-2023-0022

NUMERICAL AND EXPERIMENTAL ANALYSIS OF BALLISTIC PERFORMANCE IN HYBRID SOFT ARMOURS COMPOSED OF PARA-ARAMID TRIAXIAL AND BIAXIAL WOVEN FABRICS

Justyna Pinkos*, Zbigniew Stempien, Magdalena Małkowska

Institute of Architecture of Textiles, Lodz University of Technology, Zeromskiego 116, 90-924, Lodz, Poland
*Corresponding author. E-mail: justyna.pinkos@p.lodz.pl

Abstract:

This article presents the results of numerical and experimental research on the ballistic performance of soft packages composed of biaxial and triaxial fabrics in various hybrid configurations. The main objective of these studies was to prove the hypothesis that a hybrid package composed of biaxial fabrics, on the impact side of a projectile, and triaxial fabrics, on the backside, exhibits greater ballistic efficiency than a package entirely composed of biaxial or triaxial fabrics. The research was conducted by shooting packages consisting of 30 layers of fabrics using a Parabellum 9 × 19 full metal jacket projectile, with a striking velocity of 380 m/s, after placing the packages on a Roma No.1 plasticine substrate. The analysis involved the deformation depth of the plasticine substrate and the perforation ratio of the packages. Optimisation studies revealed that the optimal package configuration should consist of 9 layers of biaxial fabrics on the projectile impact side and 21 layers of triaxial fabrics on the backside, indicating a biaxial to triaxial fabric ratio of approximately 1:3.

Keywords:

Soft ballistic package, triaxial fabric, biaxial fabric, hybrid package arrangement, ballistic performance

1. Introduction

Bulletproof vests constitute a significant element of the protection of individuals exposed to gunfire from handguns and, when supplemented with ballistic plates, they also offer protection against rifle fire, preventing various critical injuries and, even, death [1–3]. Contemporary armed conflicts, acts of terrorism, organised criminal activities, and political strife necessitate the need for soldiers, law enforcement officers, and key figures to wear personal protection. It should be noted that the design of a bulletproof vest should feature appropriate ballistic parameters which comply with the prevailing standards [4], while ensuring user comfort through flexibility and lightness [1,5]. Ongoing research aimed at improving the effectiveness of textile-based ballistic shields primarily focusing on enhancing the strength properties of the materials used in their construction [6–8]. Concurrent with this approach, textile technologies are also being developed to devise optimal fabric structures and ballistic packages, allowing for more efficient absorption of kinetic energy from projectiles and, thus, reducing blunt injuries to the body. The latest breakthrough in fibre material enhancement is the development of a 2D poly-aramid, known by its trade name "Kevlar® EXO™," which is characterised by dense interlayer hydrogen bonds, making it more resistant to thermal degradation and possessing greater compressive strength compared to commonly used ballistic para-aramids [7]. Unpublished strength studies indicate that Kevlar® EXO™ fibres exhibit the highest ballistic performance among all previously used aramid fibres in bulletproof vests. Commonly used structures in the layers of ballistic packages include woven fabrics made from continuous para-aramid fibres and unidirectional (UD) sheets made from ultra-high molecular weight polyethylene (UHMWPE) or para-aramid fibres. Woven fabrics are most commonly fabricated in a plain weave using para-aramid yarns of various linear densities. Ballistic packages are formed from these products as multilayer structures based on accepted bulletproof vest resistance classes, ensuring effective protection based on projectile type and impact velocity. Typical studies aimed at developing woven fabrics with increased ballistic performance focus on analysing the influence of weave type [9–12], thread density of the weft and warp [13], crimp of weft and warp threads [14], areal density [15], and friction between weft and warp threads [16–18] on fabric ballistic performance. Other studies, extending beyond the mere modification of a fabric's geometric structure, involve impregnating and depositing shear thickening fluids [19–21], carbon nanotubes [22,23], or graphene oxide sheets [24] onto fabric surfaces and internal spaces. Efforts are also being made to develop entirely different structures than biaxial fabrics and UD sheets, such as embroidered structures [25,26] and triaxial fabrics [27]. In the production of embroidered structures, the tailored fibre placement technique is employed, where the main thread is computer-positioned and attached to the substrate by an affixing thread. Research has shown that such structures can significantly reduce blunt trauma when used in hybrid arrangements with woven fabrics [25,26]. A disadvantage of these structures is the significant perforation of layers due to the ease with which threads can spread upon contact with the projectile's nose [26]. In the case of multiaxial fabrics, the issue of their ballistic performance is relatively underexplored, despite the concept of producing these structures being known for many years [28–30]. The difficulty in developing high-efficiency looms for manufacturing these fabrics is one reason for this. Since around 2016, only triaxial fabrics with very limited structural and raw material parameters have been producible on a mass scale. The initial assessments of the

ballistic performance of packages composed of triaxial fabrics made from Nylon 66 polyamide threads were published in the 1980s [31]. It was hypothetically assumed that triaxial fabrics should exhibit better ballistic properties than biaxial fabrics due to their greater isotropy, leading to a more evenly distributed stress around the impact area. Comparative studies on the ballistic effectiveness of packages made from biaxial and triaxial fabrics were conducted by determining the minimum number of layers, ensuring non-penetration of the package. Based on these experimental studies, it was found that the minimum number of layers ensuring non-penetration for biaxial fabrics was 10; whereas, for triaxial fabrics, it was 14 layers under the assumed shooting conditions. The reason cited for the poorer performance of triaxial fabrics was their significantly higher openness, compared to biaxial fabrics, leading to easier penetration by projectiles. Further research on the ballistic performance of triaxial fabrics was only published in 2018 [32]. The primary aim of the study was to verify the applied material model for the para-aramid in computer simulations based on experimental results, where the deformation of biaxial and triaxial fabrics and the residual energy of the projectile were analysed. A similar modelling methodology was employed in another study, to compare the ballistic performance of packages comprising biaxial and triaxial Kevlar 29 fabrics. The ballistic packages were fixed within steel frames and subjected to Parabellum 9 × 19 full metal jacket (FMJ) bullet impacts at a striking velocity of 406 m/s [33]. The simulation and experimental studies conducted demonstrated that ballistic packages made from triaxial fabrics exhibited significantly smaller back-face deformation (BFD), compared to packages composed of biaxial fabrics. Additionally, the packages made from triaxial fabrics showed a more favourable cone-shaped deformation, which could lead to reduced ballistic trauma. However, weaker properties were noted for these packages, in terms of the minimum number of layers required to stop the projectile, which results from the open structure of triaxial fabrics. In the same research group, further experimental studies were carried out to analyse the injuries sustained by a human body protected by ballistic packages made from biaxial and triaxial fabrics during non-penetrating impacts by Parabellum 9 × 19 FMJ bullets at a velocity of 406 m/s [34]. The ballistic packages were composed of 30 layers of biaxial and triaxial fabrics with comparable areal densities and made from the same Kevlar 29 yarn. A physical model of the human body was developed, incorporating models of the heart, lungs, and musculoskeletal system, onto which the developed ballistic packages were placed. The body model was equipped with pressure sensors and signals were recorded during the shooting at various points. The studies revealed that the pressures recorded by the sensors were consistently lower when the body model was shielded by a package made from triaxial fabrics, indicating a smaller scale of behind-armour blunt trauma. It was also observed that the number of penetrated layers for the package composed of triaxial fabrics was 12, while, for the biaxial fabrics, it was 10, which can be attributed to the higher openness of the triaxial fabrics.

The research conducted to date, clearly indicates that all textile structures developed for use in ballistic packages possess both advantageous and disadvantageous properties, in terms of their ballistic performance. This is well illustrated by various comparative studies on the ballistic performance of packages, such as those composed of woven fabrics and UD sheets [35,36], biaxial and triaxial fabrics [32,33], and woven fabrics and embroidered structures [25,26]. Therefore, an intriguing direction for research is aimed at enhancing the ballistic performance of packages by using hybrid orientation of layers within the ballistic package. This approach involves assembling the package from different textile structures, to maximise the favourable properties of these structures while minimising the unfavourable ones. In hybrid ballistic packages, textile woven structures are often combined with UD structures [36–38]. Research in this area generally indicates that placing woven fabrics at the front of the hybrid package and UD structures at the back provides better ballistic protection than the reverse order. Placing fabrics on the impact side is advantageous because they have an interwoven structure that prevents threads from spreading upon contact with the projectile's nose, which beneficially limits package perforation. Conversely, positioning UD structures at the back is beneficial because they have spread-out fibres or threads that can immediately distribute high stresses upon projectile impact, aiding in reducing the BFD of the package. A similar concept has been applied in hybrid packages composed of woven fabrics and embroidered structures [26]. Studies demonstrated that the best ballistic performance was exhibited by hybrid packages containing woven fabrics on the impact side and embroidered structures with spread-out threads at the back. It was shown that in the most efficient ballistic package, the ratio of woven to embroidered layers should be 1:3.

The existing studies on the ballistic performance of triaxial fabrics have demonstrated that their drawback lies in their susceptibility to perforation upon contact with the projectile's nose because of their openness. However, their advantage lies in their greater isotropy compared to biaxial fabrics, leading to stress distribution over a larger area and more effective dissipation of kinetic energy from the projectile, which contributes to reducing the BFD of packages made from these fabrics. However, it is possible to limit the contact of triaxial fabrics with the projectile's nose by using a hybrid package structure where biaxial fabrics are positioned on the impact side. Hypothetically, a hybrid package structure could reduce the unfavourable properties of triaxial fabrics, such as their high openness, that makes them susceptible to perforation when in contact with a projectile's nose. Consequently, this ballistic package construction might result in reducing ballistic trauma by minimising the cone-shaped deformation of the ballistic package. This article presents the results of numerical and experimental studies on the ballistic performance of soft packages comprising biaxial and triaxial fabrics in various hybrid configurations. The main objective of these studies was to prove the hypothesis that a hybrid package composed of biaxial fabrics on the impact side possesses greater ballistic efficiency than a package entirely composed of biaxial or triaxial fabrics. The research involved shooting packages with Parabellum 9 × 19 FMJ bullets at a striking velocity of 380 m/s, after placing the packages on a Roma No.1 plasticine substrate. The analysis included the depth of deformation of the plasticine substrate and the perforation ratio (PR) of the packages. Additionally, an optimisation process was conducted to define the structure of the package with the best ballistic performance.

Table 1. Detailed structural parameters of biaxial and triaxial Kevlar® 29 fabrics

Weave type	Thread density (threads/cm)				Areal mass (g/m^2)	Fabric thickness (mm)
	Weft	Warp	Warp +60°	Warp −60°		
Plain	7	7	—	—	200 ± 10	0.28 ± 0.03
Basic triaxial	4	—	4	4	198 ± 10	0.26 ± 0.03

2. Materials

The experimental research utilised two para-aramid fabrics: biaxial (Changzhou Utek Composite, China) and triaxial (Triaxial Structures, USA). Both fabrics were made from identical "Kevlar® 29 1500 dtex" para-aramid yarn. The detailed structural parameters of these fabrics are presented in Table 1.

For the numerical and experimental studies, four variants of ballistic packages were prepared (Figure 1). The soft ballistic packages consisted of 30 layers and measured 20 cm × 20 cm. The packages were arranged as follows: V1 – 30 layers of triaxial fabric (Figure 1a), V2 – 30 layers of biaxial fabric (Figure 1b), V3 – 15 layers of triaxial fabric on the impact side and 15 layers of biaxial fabric at the back (Figure 1c), V4 – 15 layers of biaxial fabric on the impact side and 15 layers of triaxial fabric at the back (Figure 1d). Variants V1 and V2 were created for the direct comparison of the ballistic properties of packages composed entirely of biaxial and triaxial fabrics and to verify the material models adopted in the numerical studies. The hybrid layer arrangement in the packages of variants V3 and V4 was designed to investigate whether there was a possibility to enhance the ballistic efficiency of such packages, compared to those composed entirely of biaxial fabric (Variant V2) or entirely of triaxial fabric (Variant V1).

3. Methodology of numerical and experimental research

Finite element analysis was conducted using LS-Dyna software for the numerical studies. Both numerical and experimental analyses focused on the ballistic effectiveness of packages measuring 20 cm × 20 cm, placed on a standardised plasticine substrate. The packages were assumed to have been shot by a

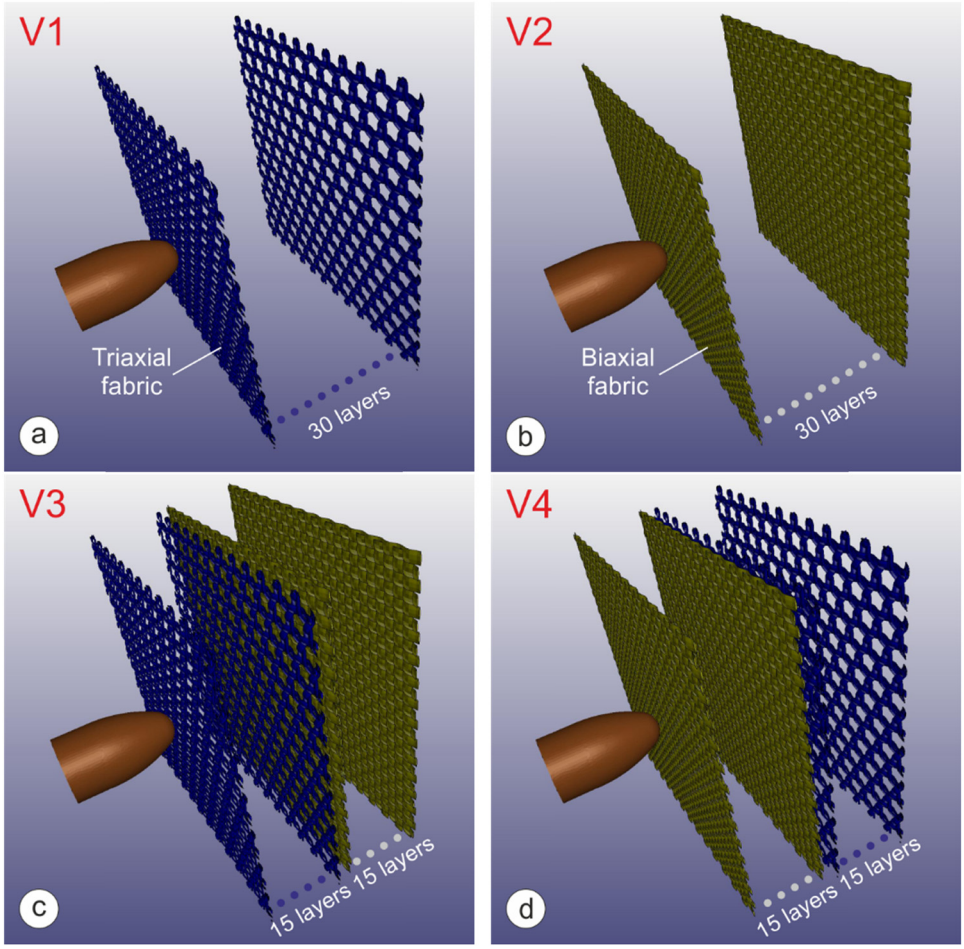

Figure 1. Variants of prepared ballistic packages: (a) Variant 1, (b) Variant 2, (c) Variant 3, and (d) Variant 4.

single shot precisely at their centre. The dimensions of the packages were chosen so that the dimensions of the cavity in the plasticine were significantly smaller than the package dimensions. Preliminary numerical and experimental investigations revealed that the base of the cone in the plasticine for the proposed package variants could inscribe a circle with a diameter of up to 10 cm. Therefore, the package size of 20 cm × 20 cm was adopted to minimise the influence of boundary conditions on the formation of the deformation cone and to maintain a certain area of zero transverse deformations around the cone at the moment of projectile stopping. The numerical model of the fabric for simulating ballistic packages is usually prepared in the form of a woven structure composed of homogenised thread structures [39–41]. Due to the significantly smaller transverse dimensions of the threads compared to the ballistic package dimensions, the number of finite elements in such a model is very high, posing a computational challenge even with efficient computer systems. Therefore, when modelling package layers as woven structures, smaller package dimensions were used, typically up to 10 cm [42–46], or between 10 and 15 cm [47–49], or, rarely, from 15 to 20 cm [26,33,50,51]. Besides the number of finite elements in the model, the simulation time is a significant factor affecting computational duration. A projectile impacting a soft ballistic package usually stops within 100–150 μs [26,33,52]. In cases where the package was placed on a plasticine substrate and the deformation of this substrate was examined, the computational time significantly extended due to the shockwave generated in the plasticine during projectile impact, affecting the final substrate deformation. Simulation studies indicate that this time can extend up to 1,000 μs because of the shockwave [53].

Preliminary simulation studies of ballistic packages measuring 20 cm × 20 cm, comprising biaxial and triaxial fabrics, maintaining woven structures in the layers as described in the study by Gloger et al. [26], and placed on a plasticine substrate, indicated that for a simulation time of 1,000 μs, the computational time could exceed 1 year, even if a Hewlett-Packard HP Z8 G4 workstation with 24 cores was used. Due to an extensive research plan, involving calculations for multiple package variants, this time frame was not acceptable. Therefore, simplified 2D homogeneous layer models were adopted for the simulation studies. Such a simplification of layers is sometimes applied in the examination of ballistic packages with larger dimensions, exceeding 12 cm × 12 cm [39,54,55], or in hybrid models where the impact area is modelled using woven structures typically sized up to 8 cm × 8 cm, while the remaining part is simulated using 2D shells or thin homogenised 3D structures [46,56,57]. Based on these assumptions, the models for biaxial and triaxial fabrics were generated as 2D shell elements (20 cm × 20 cm) with hexa/shell finite elements and edge dimensions up to 2.5 mm (Figure 2a). The thickness of the 2D shell elements in the numerical calculations was determined based on the surface mass of Kevlar® 29 1500 dtex biaxial and triaxial fabrics and a para-aramid density of 1,440 kg/m³. To balance the surface mass of biaxial and triaxial fabrics, a shell thickness of 0.14 mm was assumed in the computations. In the subsequent stage of the research, a numerical model was prepared from the developed layers, constituting a package composed of 30 layers (Figure 2b). For the investigations, the packages were subjected to the impact of a Parabellum 9 × 19 mm FMJ bullet. This bullet is recommended by most certification standards for ballistic vests. The well-known NIJ 0101.06 standard suggests this type of bullet for certification tests for all protection levels (IIA, II, and IIIA) intended for bulletproof vests with textile inserts [4]. The model of this bullet was created based on actual dimensions (Figure 2c). Separate models were developed for the jacket and the core of the bullet, for which finite element meshes of tetra/solid types with edge dimensions up to 0.2 mm were generated. In the final phase, a model of a plasticine block, with dimensions of 20 cm × 20 cm × 14 cm, was developed, for which a finite element mesh of tetra/solid types with gradient-changing edge dimensions was generated. The smallest elements, with edge dimensions up to 1 mm, were concentrated at the point of impact of the bullet. From this point, the elements

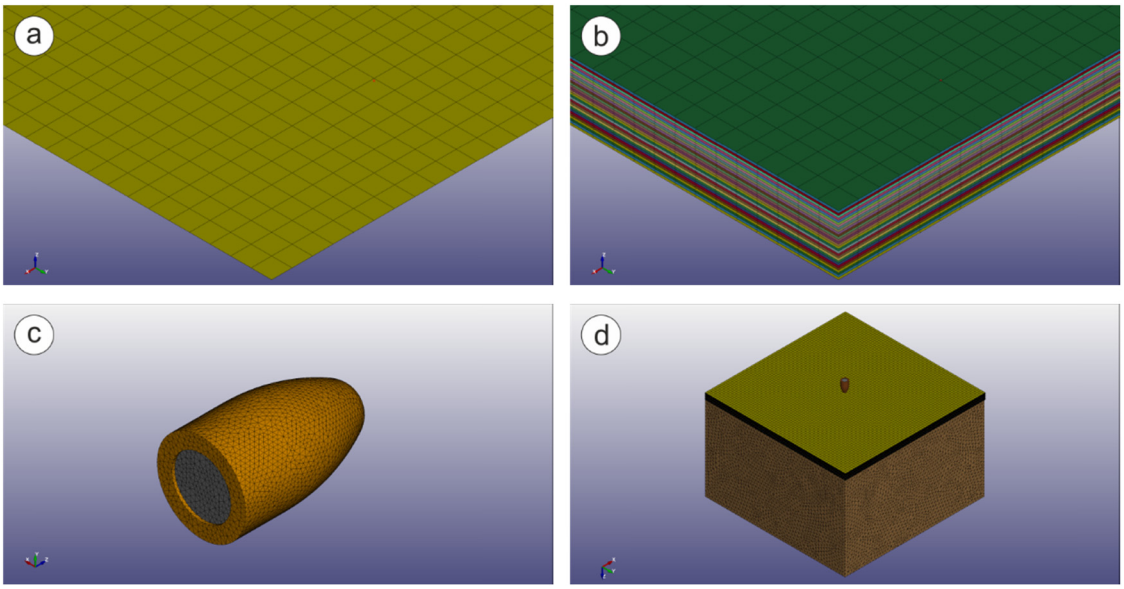

Figure 2. Numerical model: (a) single layer, (b) ballistic package containing 30 layers, (c) Parabellum 9 × 19 mm FMJ bullet, and (d) complete numerical model.

gradually increased in size, reaching edge dimensions of up to 10 mm on the rear and side walls of the block. These ballistic package models (consisting of 30 layers of fabric, the Parabellum 9 × 19 FMJ bullet, and the plasticine block) were combined to form a complete model ready for numerical calculations (Figure 2d). The number of layers in the biaxial fabric package was determined based on preliminary experimental studies, so that when the package was placed on a plasticine substrate and shot by a Parabellum 9 × 19 FMJ bullet at an impact velocity of 380 m/s, the maximum deformation of the substrate was less than 44 mm, following the NIJ 0101.06 standards. Present recommendations aim for this value to be even lower than the established standard. Therefore, the number of layers in the package was chosen so that the maximum deformation of the plasticine substrate reached approximately 80% of the allowable value, corresponding to an allowable deformation of around 35 mm. Preliminary studies indicated that such a deformation level could be achieved for a package comprising the 30 layers of Kevlar 29 biaxial fabrics chosen for this study.

To determine the ballistic effectiveness of packages made of biaxial and triaxial fabrics in numerical studies, two different material models were employed, maintaining identical strength parameters. Anisotropic properties of the biaxial fabric were achieved by adopting the *MAT_ORTHO_ELASTIC_PLASTIC material model for the finite elements. Material coordinates within the finite elements were oriented so that coordinate “a” aligned with the direction of the warp threads and coordinate “b” aligned with the direction of the weft threads. The parameter values for the model were adopted based on published data [58] (Table 2). To define the failure criterion and erasing of finite elements, an additional material setting card *MAT_ADD_EROSION was implemented. In this card, the failure strain value was set at 3.6%, which is consistent with Kevlar 29 para-aramid [58].

Regarding the triaxial fabric within the material model library of LS-Dyna, there are no models available for a material exhibiting mechanical properties dependent on three directions. Therefore, considering the quasi-isotropic properties of Kevlar 29 triaxial fabric, the material model *MAT_PLASTIC_KINEMATIC was adopted. The accepted parameter values for this material model are presented in Table 3 [58].

For the Parabellum 9 × 19 FMJ bullet, the same *MAT_SIMPLIFIED_JOHNSON_COOK material model was used for both the bullet’s lead core and its ballistic brass jacket. Table 4 shows the model parameter values for the lead core, while Table 5 shows the values for the ballistic brass jacket [26,33].

In the case of the Roma No. 1 plasticine backing material, the *MAT_ POWER_ LOW_ PLASTICITY material model was adopted, which is commonly used in numerical studies for this backing material [59–61]. The accepted parameter values for this model are presented in Table 6, determined through dynamic indentation tests [59].

In the numerical studies, the AUTOMATIC_SURFACE_TO_SURFACE contact type was utilised, while accounting for the dynamic friction coefficients μ_d and static friction coefficients μ_s between adjacent shells (μ_d = 0.2, μ_s = 0.2 [16,62,63]), jacket and bullet core (μ_d = 0.8, μ_s = 0.8 [16,62,63]), jacket and successive layers of the package (μ_d = 0.28, μ_s = 0.3 [16,62,63]), bullet core and successive layers of the package (μ_d = 0.28, μ_s = 0.3 [16,62,63]), and package shells and the ballistic clay (μ_d = 0.9, μ_s = 0.9 [64]).

Table 2. Parameter values utilised in the *MAT_ORTHO_ELASTIC_PLASTIC material model for the biaxial fabric

Density RO (kg/m^3)	Young’s modulus E_1 (GPa)	Young’s modulus E_2 (GPa)	Poisson’s ratio PR_1	Poisson’s ratio PR_2	Yield stress SIGY (MPa)
1,440	70	70	0.3	0.3	2.75

Table 3. Parameter values utilised in the *MAT_PLASTIC_KINEMATIC material model for the triaxial fabric

Density RO (kg/m^3)	Young’s modulus *E* (GPa)	Poisson’s ratio PR	Yield stress SIGY (MPa)	Failure strain FS (%)
1,440	70	0.3	2.75	3.6

Table 4. Parameter values utilised in the *MAT_SIMPLIFIED_JOHNSON_COOK material model for the lead core

Density RO (kg/m^3)	Young’s modulus *E* (GPa)	Poisson’s ratio PR	Constant *A*	Constant *B*	Constant *N*	Constant *C*
11,300	1	0.42	$5 \times 10^{+6}$	$4 \times 10^{+7}$	0.5	0.628

Table 5. Parameter values utilised in the *MAT_SIMPLIFIED_JOHNSON_COOK material model for the ballistic brass jacket

Density RO (kg/m^3)	Young’s modulus *E* (GPa)	Poisson’s ratio PR	Constant *A*	Constant *B*	Constant *N*	Constant *C*
8,941	130	0.375	$112 \times 10^{+6}$	$5{,}050 \times 10^{+5}$	0.42	0.009

Table 6. Parameter values utilised in the * MAT_POWER_LOW_PLASTICITY material model for the Roma No. 1 clay [59]

Density RO (kg/m^3)	Young's modulus *E* (MPa)	Poisson's ratio PR	*K* (kPa)	*N*
1,529	11.64	0.49	153	0.181

The experimental investigation of ballistic package effectiveness was conducted by placing the packages on a standardised Roma No. 1 plasticine substrate and shooting them with Parabellum 9 × 19 FMJ bullets. To achieve this, a box measuring 400 mm × 400 mm × 140 mm was filled with Roma No. 1 plasticine. The plasticine underwent calibration by maintaining it at a specified stabilised temperature and baking it for 24 h. After removal, a 63.5 mm diameter, 1,043 g steel ball was dropped from a height of 2 m onto the surface at five locations. Using a calliper, the maximum depth of the clay deformation, concerning the zero reference surface, was measured at each ball drop point. The experiments were conducted at three different temperatures. Figure 3 illustrates the relationship between the maximum deformation of the ballistic clay substrate and the heating temperature. The experimental results were fitted with an exponential function (1).

$$D_p(T) = D_{p0} + D_{p1} \times \exp\left(\frac{T - T_0}{T_1}\right). \quad (1)$$

The values of individual parameters of the fitting function were D_{p0} = 8.97, D_{p1} = 2.18, T_0 = 29.25, and T_1 = 4.42. The calculated coefficient of determination (R^2) during the fitting was 0.997, indicating a very good fit of the fitting function to the measurement data.

According to the standards [4], for a properly calibrated plasticine substrate, the average maximum deformation value for five drop points should be 19 ± 2 mm. Based on the equation of the fitting function (1), the heating temperature of the plasticine substrate was determined using equation (2).

$$T = T_1 \times \ln\left(\frac{D_p - D_{p0}}{D_{p1}}\right) + T_0. \quad (2)$$

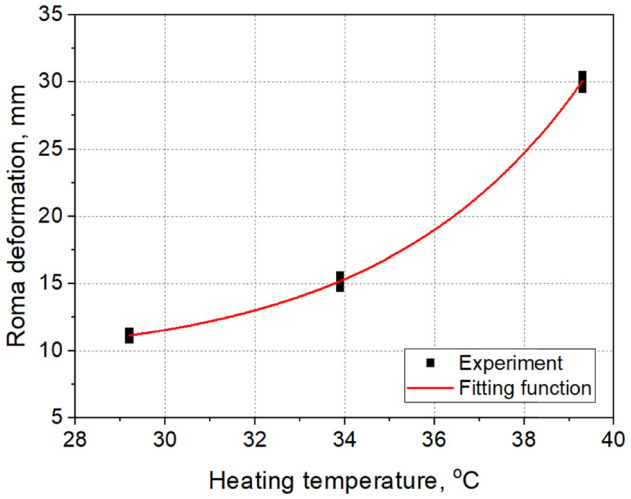

Figure 3. Maximum deformation of the plasticine substrate as a function of heating temperature.

After substituting the data into equation (2), the heating temperature of the plasticine substrate was calculated as 36.1°C, at which the maximum depth of deformation after dropping the ball should be 19 mm. Subsequently, the plasticine substrate was heated in an oven at 36.1°C, and a ball was dropped onto the heated substrate. The average maximum deformation value at five drop points was measured at 19.3 ± 0.5 mm, which was considered to be consistent with the recommendations outlined in the standards. Based on this, it was established that, before each shot, the plasticine substrate would be heated at 36.1°C for 24 h.

The ballistic testing of the packages was conducted at the Ballistic Research Laboratory using the setup shown in Figure 4. A ballistic gun (1) was used to fire a projectile (2), which then passed through a set of gates (4) measuring its velocity. The projectile was stopped by the ballistic package (5), secured with special straps on a box filled with plasticine (6). The tests were performed using Parabellum 9 × 19 mm FMJ bullets (Sellier & Bellot, Vlasim, Czech Republic). For each variant, two ballistic packages were tested, each subjected to a single shot aimed at the centre of the package.

The deformation area of the plasticine substrate after the ballistic package was fired was scanned using a laser sensor station equipped with an Omron ZX1 laser sensor (Omron, Japan). Positioning in the *XY* axes was controlled using linear drives with stepper motors (Figure 5).

The process of scanning the plasticine base involved moving the laser distance sensor along successive scan lines using linear drives and measuring the depth of deformation. Measurements were taken at 0.5 mm intervals. A NI USB6255 measurement card (National Instruments, USA) and software developed in Visual Studio programming language were used to control the operation of the linear drives and measure the depth of deformation. Each time, an area of 18 cm × 18 cm was scanned, with the

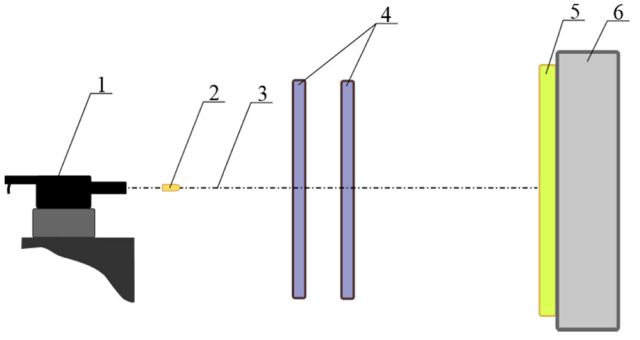

Figure 4. Schematic of the ballistic tunnel: 1 – ballistic gun, 2 – projectile, 3 – projectile flight path, 4 – array of gates for measuring projectile impact velocity, 5 – soft ballistic package, and 6 – box filled with plasticine.

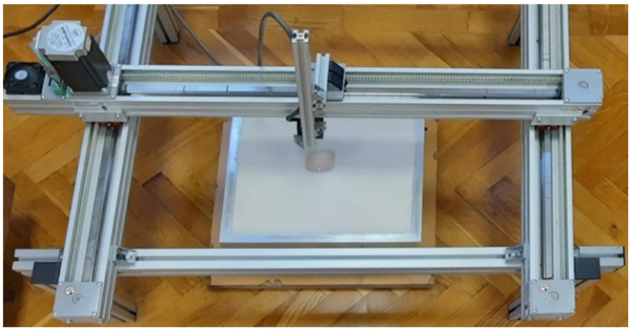

Figure 5. Station for scanning the deformation of the plasticine base using a laser distance sensor.

central point always set at the location of the deepest depression in the plasticine base. For each package after shooting, the PR was calculated using the following equation:

$$PR = \frac{N_p}{N_t} \times 100\%, \quad (3)$$

where N_p is the number of penetrated layers in the ballistic package and N_t is the total number of layers in the ballistic package.

4. Results of numerical and experimental research

Figure 6 presents the deformation of the Roma plasticine after firing package variants 1–4. The time changes in substrate deformation at the point of projectile impact, obtained from the simulation studies, are shown in Figure 6a. They reveal that substrate deformation increases over time, from about 30 µs to 1.5 ms up to a maximum value and remains at that level thereafter. Comparing packages made entirely from triaxial fabrics (Variant 1) and biaxial fabrics (Variant 2) at 2 ms, the substrate deformation after firing the package made from triaxial fabrics was lower, at 25.6 mm, compared to 32.2 mm for the biaxial fabric package. Similar dependencies were observed in the experimental studies. Figure 6b illustrates the plasticine substrate deformation in the cross-section covering the point of projectile impact obtained using the scanner shown in Figure 5. For these variants, the substrate deformation was 26.5 ± 0.8 and 34.7 ± 0.6 mm, considering the average values from two firings for each variant. The obtained results of substrate deformation at the projectile impact point in the experimental studies align closely with the results obtained in the simulation studies. The lower substrate deformations, for the package composed of triaxial fabrics, are the result of the different structures of these fabrics compared to biaxial fabrics. Triaxial fabrics primarily possess three interlaced thread systems, distributing stress over a larger fabric surface. In the case of biaxial fabrics, stress propagates in two thread systems of the weft and warp, predominantly involving threads in contact with the projectile head. Similar comparative studies after firing packages composed of triaxial and biaxial fabrics fixed in steel frames revealed that the maximum height of deformation cones is smaller for packages with triaxial fabrics [33]. In experimental studies, after firing packages composed of 30 layers of triaxial and biaxial Kevlar 29 fabrics, the maximum deformation cone heights were 33 and 48 mm, respectively.

The PR for the examined ballistic packages is presented in Figure 7a. The chart shows that the package composed of triaxial fabrics (Variant 1) shows a significantly higher PR, approximately 33.3%, compared to the package composed of biaxial fabrics (Variant 2), which measured at 16.7%. The reason for this lies in the substantial openness of the triaxial fabrics. The characteristic hexagonal openings in the triaxial fabric used in the study may have a diagonal length of about 2 mm (Figure 7b). This implies that a 9 mm diameter bullet makes direct contact with seven of these openings, likely contributing to the spreading of the threads in contact with the bullet's nose and facilitating the penetration of such fabrics. This differs from the case of biaxial fabrics, where the structure shows almost no openness and, additionally, the plain weave in these fabrics ensures the complete entanglement of both warp and weft threads, preventing the spreading of threads in contact with the bullet's nose. This significantly contributes to a

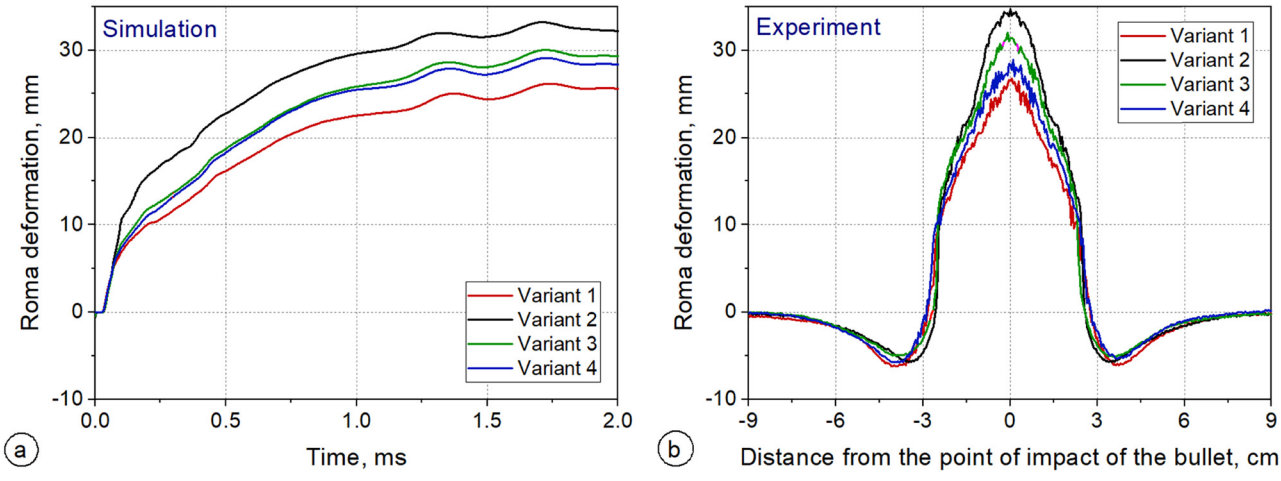

Figure 6. Plasticine substrate deformation for the tested package variants: (a) substrate deformation at the projectile impact point over time (simulation studies). (b) Substrate deformation in the cross-section covering the point of projectile impact (experimental studies).

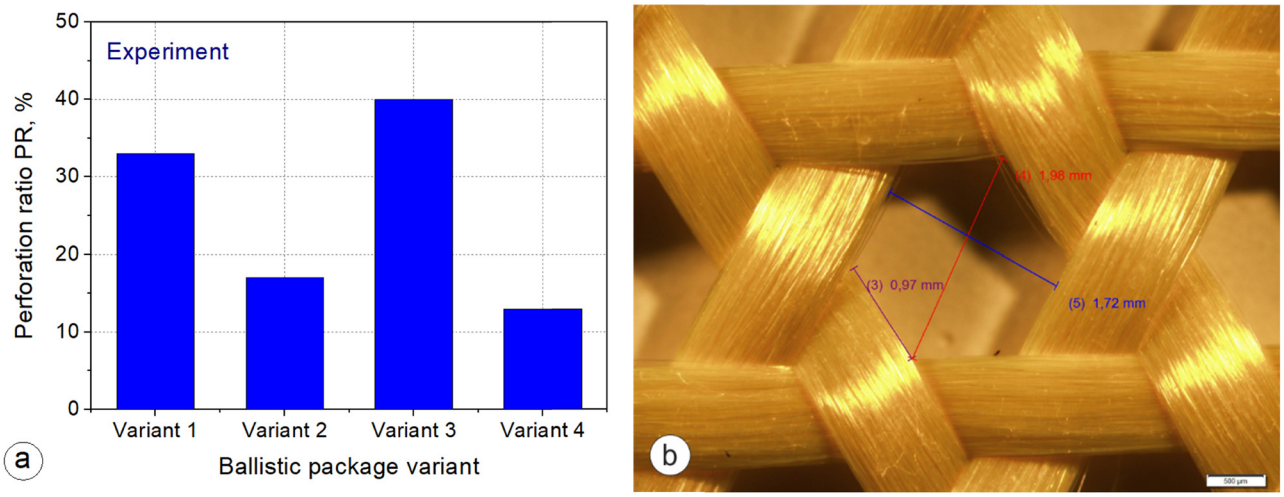

Figure 7. (a) PR of ballistic packages after being shot with bullets in experimental studies. (b) Dimensions of openings in triaxial fabric.

much lower number of penetrated layers compared to packages composed of triaxial fabrics.

Thus, it should be stated that triaxial fabrics, in terms of their response to ballistic impact, essentially have one advantage and one disadvantage. The advantage of the three systems of threads is that they cause stress waves to spread over a larger fabric area, resulting in less transverse deformation of the ballistic package. The drawback of these fabrics is their significant openness resulting from the weaving method of three systems of threads. This openness leads to thread spreading upon contact with the projectile's nose, which adversely affects the number of penetrated layers in the ballistic package. On the other hand, biaxial fabrics, concerning their response to ballistic impact, possess advantages and disadvantages that are contrary to the advantages and disadvantages of triaxial fabrics. The advantage is the interlocking structure created by the weaves of the weft and warp threads, preventing thread spreading upon contact with the projectile's nose, favouring a smaller number of penetrated layers. However, the disadvantage of this structure, compared to triaxial fabrics, is the presence of two systems of threads, causing the spread of stress waves over a smaller fabric area, and thus, significantly increasing the transverse deformation of a package composed of these fabrics. To harness the advantages of both structures, while mitigating their disadvantages, it seems appropriate to create a multi-layer hybrid package. This package would include biaxial fabrics at the front and triaxial fabrics at the back. Figure 6a and b show the deformation of a plasticine substrate for such a ballistic package (Variant 4), comprising 15 layers of biaxial fabrics at the front and 15 layers of triaxial fabrics at the back. It is evident that the maximum deformation is only slightly greater than that of a package comprising 30 layers of triaxial fabrics (Variant 1) and the PR is even lower than that of a package comprising 30 layers of biaxial fabrics (Variant 2), standing at only 13.3% (Figure 7a). Conversely, a highly disadvantageous configuration, accentuating the drawbacks of biaxial and triaxial fabrics, is a hybrid package containing triaxial fabrics at the front and biaxial fabrics at the back. Figure 6a and b show the deformation for a package made from Variant 3, with 15 layers of triaxial fabrics at the front and 15 layers of biaxial fabrics at the back. The maximum deformation was greater than in the case of shooting the package in the reverse configuration (Variant 4) and

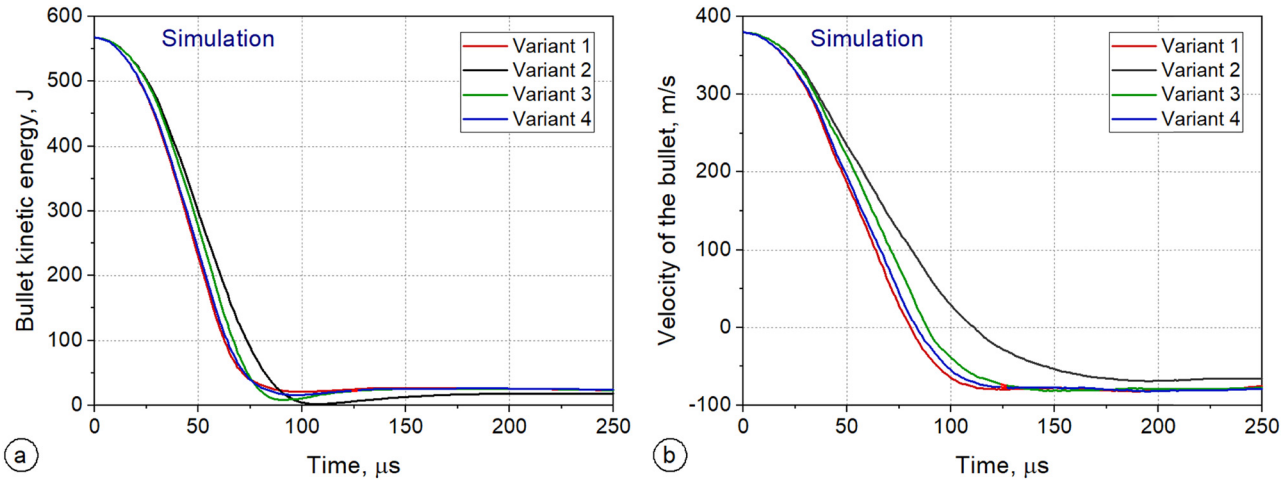

Figure 8. Simulation studies of adopted package variants: (a) kinetic energy of the projectile as a function of time and (b) projectile velocity as a function of time.

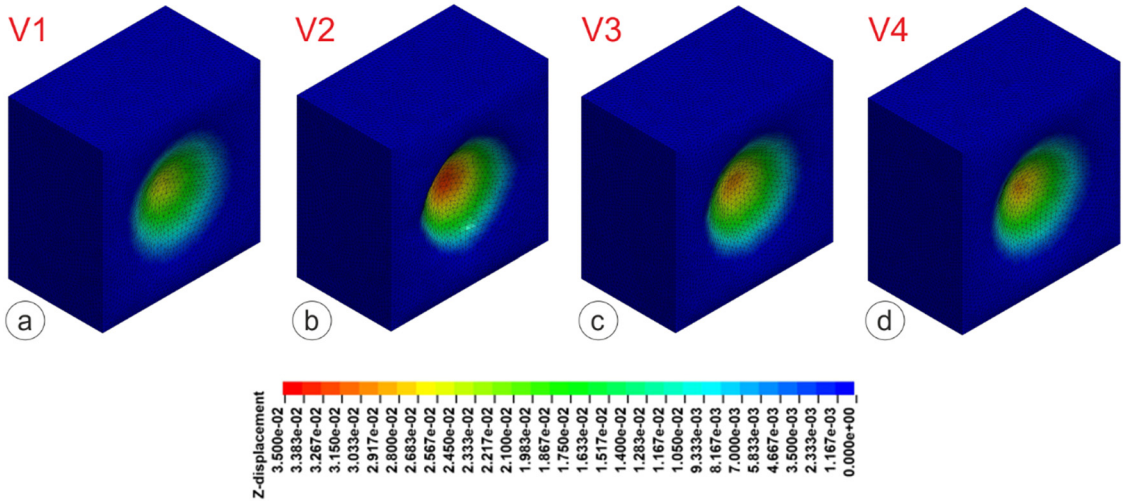

Figure 9. View of the deformation in the plasticine substrate 2 ms after shooting the ballistic package with a projectile in the simulation studies: (a) Variant 1, (b) Variant 2, (c) Variant 3, and (d) Variant 4.

the PR was also the highest, reaching 40% (Figure 7a). This implies that the projectile penetrated through 12 initial layers. The response of hybrid packages produced in Variants 3 and 4 confirms the existence of advantages and disadvantages of triaxial and biaxial fabrics. However, proper management of these materials can significantly enhance the ballistic properties of the packages.

Figure 8a and b shows the kinetic energy of the projectile and its velocity as a function of time, for the studied package variants. Simulation studies clearly show that using triaxial fabrics in ballistic package structures results in faster projectile deceleration compared to using only biaxial fabrics. The projectile decelerates most rapidly in the case of shooting the hybrid package made in Variant 4, with this deceleration taking approximately 80 µs. Conversely, the longest deceleration time of the projectile, about 110 µs, occurs in the case of shooting the package made in Variant 2, which only comprises biaxial fabrics. The hybrid arrangement in Variant 4 is the most efficient for two reasons. First, the presence of biaxial fabrics on the impact side significantly reduces the number of penetrated layers. Second, the presence of triaxial fabrics at the back distributes stress over a larger area, effectively increasing the intensity of kinetic energy dissipation from the projectile.

Figure 9 presents views of the deformation in the plasticine substrate 2 ms after shooting the ballistic package with a projectile obtained in simulation studies for the investigated package variants. Meanwhile, in Figure 10 (for the investigated package variants), views of the deformation in the plasticine substrate after shooting these packages in experimental studies are shown. Simulation and experimental studies both indicate that, in the case of shooting a package composed entirely of biaxial fabrics (Variant 2), the maximum substrate deformation is the highest. The area of the plasticine substrate affected by non-zero deformation is slightly larger in the simulation studies than in the experimental studies. This is due to the substantial simplification of numerical models adopted for biaxial and triaxial fabrics, in the form of shells.

In the simulation studies, the entry craters for package variants containing triaxial fabrics (V1, V3, and V4) have a circular shape (Figure 9a, c, and d); whereas, in the experimental studies, the entry crater shape appears hexagonal (Figure 10a, c, and d), which is typical for triaxial fabrics. The circular distribution of deformation obtained in simulation studies for packages involving triaxial fabrics results from the adoption of the material model *MAT_PLASTIC_KINEMATIC for finite elements in the numerical model of these fabrics, generating an isotropic stress

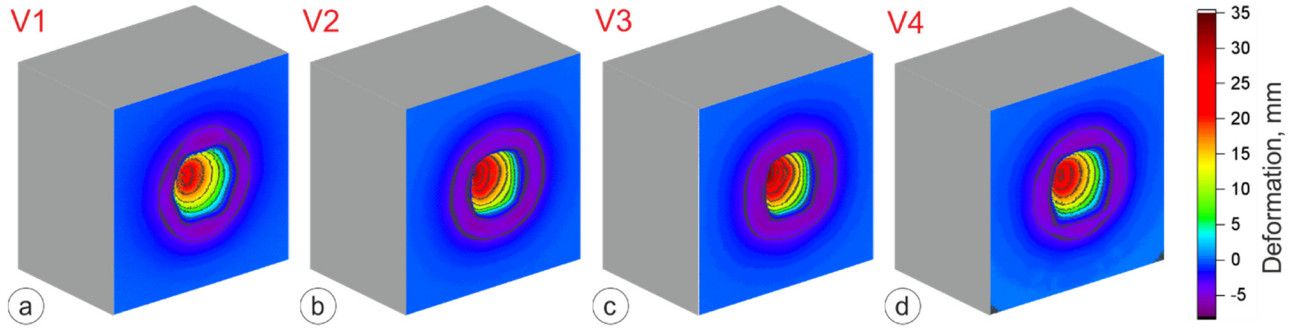

Figure 10. View of the deformation in the plasticine substrate after shooting the ballistic package with a projectile in experimental studies: (a) Variant 1, (b) Variant 2, (c) Variant 3, and (d) Variant 4.

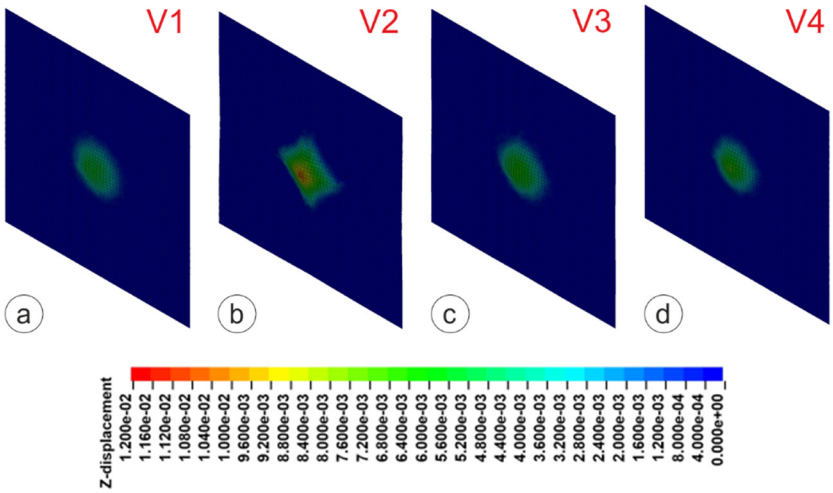

Figure 11. View of the deformation on the backside of the ballistic package after shooting, at the moment of projectile stopping: (a) Variant 1, (b) Variant 2, (c) Variant 3, and (d) Variant 4.

distribution. In the case of shooting the package made from Variant 2, in experimental studies, the shape of the entry crater is closer to a square (Figure 10b), having characteristics of biaxial fabrics and resulting from a biaxial stress distribution. In simulation studies, this shape is not entirely replicated (Figure 9b), despite the adoption of the material model *MAT_ORTHO_ELASTIC_PLASTIC for finite elements in the numerical model of these two-axis fabrics, which generates an anisotropic stress distribution.

Figure 11 shows the deformation of the last 30 layers of the ballistic package at the moment that the projectile was stopped, for all investigated variants of ballistic packages. It should be noted that, in the case of packages containing triaxial fabrics, the distribution of deformation around the point of projectile impact is circular (Figure 11a, c, and d), while for a package entirely composed of biaxial fabrics, the deformation distribution is approximately square (Figure 11b), resulting from the anisotropic structure of these fabrics. The maximum transverse deformation is highest for the package made from Variant 2 and lowest for the package made from Variant 4. These values are 10.1 and 6.2 mm, respectively. It is worth noting that these values are significantly lesser than the maximum transverse deformations of the plasticine substrate after shooting these packages. Figure 12 presents the deformation of the plasticine substrate and the last (30th) layer of the package at the point of projectile impact on a common graph, as well as the projectile nose displacement during the shooting of the package made in Variant 2.

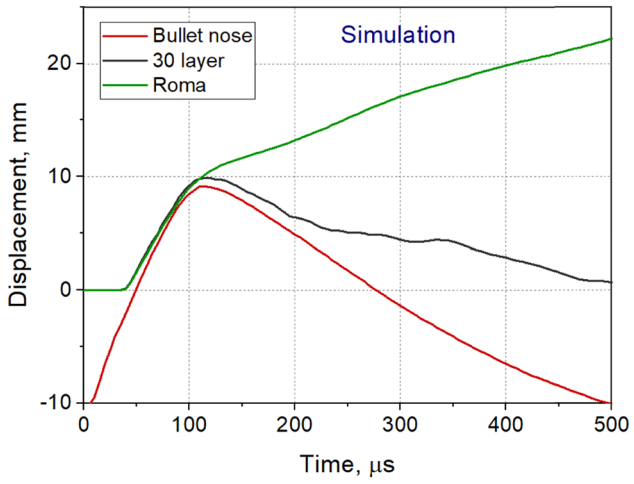

Figure 12. Displacement of the projectile nose, the last layer of the package, and the plasticine substrate at points along the projectile's flight path, after shooting the package made from Variant 2.

From the moment the impacting projectile touches the first layer of the package, the destruction and degradation of subsequent layers occur, and the transverse wave begins to propagate within the final layer of the package after approximately 30 μs. After this time, the displacement of the projectile, along with the deformation of the last (30th) layer of the package, and the plasticine substrate along the projectile's flight path, align. At around 120 μs, the projectile comes to a stop, while the transverse deformation of the 30th layer reaches a maximum of approximately 10 mm and gradually decreases in subsequent time intervals. The situation is different for the plasticine substrate, where the deformation continues to increase but with reduced intensity, reaching approximately 32 mm at around 1.5 ms, and remaining relatively constant thereafter (Figure 6a). This is due to the propagation of the shock wave, which causes the displacement of the clay substrate even when the projectile nose and the final layer of the ballistic package along the projectile's flight path have already stopped and subsequently gone back. Similar trends were observed in simulation studies during the impact of a 7.62 × 25 mm FMJ projectile on a multilayer package composed of UHMWPE laminates and a ceramic plate [53]. These studies demonstrated that the BFD of the package reached a maximum value of approximately 5 mm after about 100 μs, while the substrate continued to deform, reaching approximately 20 mm after 1 ms, due to the generated shock wave.

Research conducted on ballistic packages made from Variants 1 through 4 indicated that the most significant ballistic effectiveness is demonstrated by the package created from Variant 4,

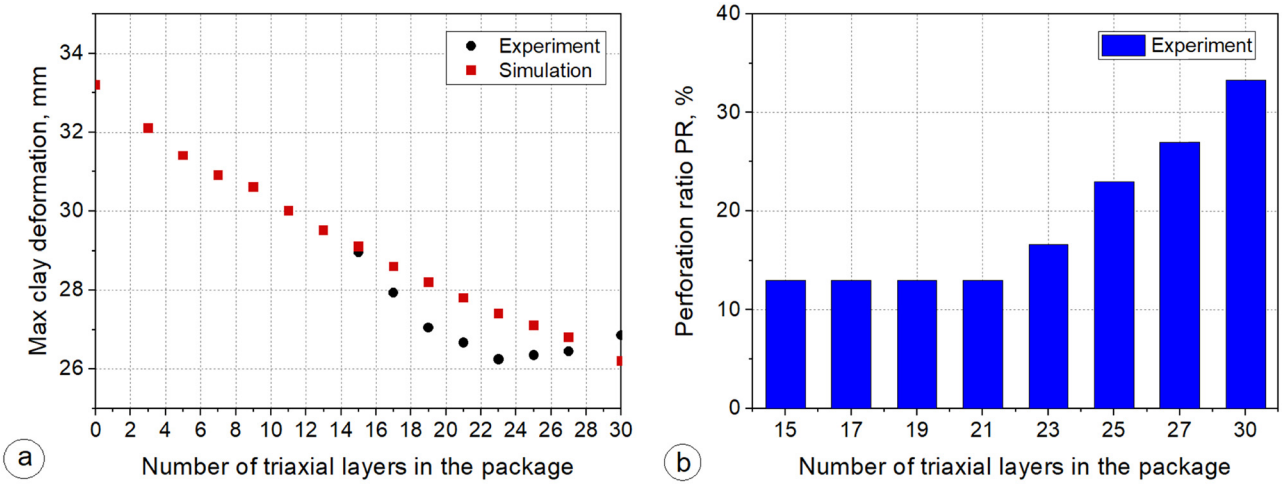

Figure 13. The influence of the number of layers of triaxial fabrics on: (a) plasticine substrate deformation and (b) PR of the ballistic package.

comprising 15 layers of biaxial fabrics on the impact side and 15 layers of triaxial fabrics on the rear side. This package, both in simulation and experimental studies, is the fastest in stopping the projectile, has the lowest layer PR, and when this package is shot, the plasticine substrate only shows slightly higher transverse deformation compared to shooting a package made entirely of triaxial fabrics (Variant 1). In turn, this exhibits a notably high PR. Further investigations were conducted to find the optimal structure of a package comprising biaxial fabrics on the front and triaxial fabrics on the rear. The objective function considered the relationship between the maximum deformation of the plasticine substrate and the number of layers of triaxial fabrics in the ballistic package. Through numerical and experimental studies, such a package configuration was sought, in order to minimise this function.

Figure 13a illustrates the numerical and experimental studies on the influence of the number of layers of triaxial fabrics in a ballistic package consisting of 30 layers, where the triaxial fabrics are placed at the rear, on the plasticine substrate deformation at the point of projectile impact. In numerical studies, there is an approximately linear decrease in the maximum clay substrate deformation with an increase in the number of layers of triaxial fabrics in the package. In the case of experimental studies, the decrease in substrate deformation was observed until the number of triaxial fabric layers in the package reached 23. Further increases in the number of triaxial fabric layers resulted in a slight increase in the maximum plasticine substrate deformation. The difference between numerical and experimental results arises from the simplified numerical models used for both biaxial and triaxial fabrics. The use of these simplified models was needed due to the computational limitations of the available workstation. On the other hand, Figure 13b presents experimental studies on the relationship between the PR and the number of layers of triaxial fabrics in a ballistic package consisting 30 layers. The research demonstrates that the lowest PR, at 13.3%, occurs in packages containing at least nine layers of biaxial fabrics on the impact side. Further reductions in the number of biaxial fabric layers and simultaneous increases in the number of triaxial fabric layers lead to a gradual increase in the PR, reaching 33.3% for a package entirely composed of triaxial fabrics. Considering the influence of the number of triaxial fabric layers on plasticine substrate deformation and the PR, the optimal structure for the ballistic package should comprise 9 layers of biaxial fabrics on the impact side and 21 layers of triaxial fabrics at the rear.

5. Conclusion

Triaxial fabrics, used in soft ballistic packages during testing with a plasticine substrate, show significantly less deformation of the substrate, compared to packages made of biaxial fabrics, considering the same type of yarn from which these fabrics were made and the same surface mass of both types of fabrics. The disadvantage of triaxial fabrics is the high and unacceptable perforation of the package during shooting, which, in turn, is at a very low level in the case of biaxial fabrics. This results from the open structure of triaxial fabrics; whereas, biaxial fabrics designed for ballistic packages do not have any openness and the interlocked warp and weft threads effectively prevent the threads from spreading upon contact with the projectile's nose. It is possible to construct a ballistic package that ensures plasticine substrate deformation at the level achieved for a package entirely composed of triaxial fabrics, while simultaneously maintaining a PR similar to that of a package composed entirely of biaxial fabrics, through a hybrid arrangement of layers. Research has shown that such performance is achieved by a package containing biaxial fabrics on the impact side of the projectile and triaxial fabrics on the rear side. Optimisation studies have shown that the best package arrangement should consist of 9 layers of biaxial fabrics on the projectile impact side and 21 layers of triaxial fabrics on the rear, indicating a ratio of biaxial to triaxial fabrics of approximately 1:3. The conducted research indicated that the development of multi-axis fabrics could be an interesting direction in the development of more efficient ballistic packages. It seems that a significant problem to solve would be the development of multi-axis fabrics, which significantly reduces openness, compared to the triaxial fabrics used in the research presented here.

Conflict of interest: Authors state no conflict of interest.

References

[1] Abtew, M. A., Boussu, F., Bruniaux, P. (2021). Dynamic impact protective body armour: A comprehensive appraisal on panel engineering design and its prospective materials. Defence Technology, 17(6), 2027–2049.

[2] Latourrette, T. (2010). The life-saving effectiveness of body armor for police officers. Journal of Occupational and Environmental Hygiene, 7(10), 557–562.

[3] Liu, W., Taylor, B. (2017). The effect of body armor on saving officers' lives: An analysis using LEOKA data. Journal of Occupational and Environmental Hygiene, 14(2), 73–80.

[4] Department of Justice, USA, Ballistic Resistance of Body Armor, NIJ Standard-0101.06. (2012).

[5] Perry, A. (2018). Ballistic-resistant body armor: Problems and coping strategies. Journal of Textile and Apparel, Technology and Management, 10(4), 1–14.

[6] Gaikwad, V. (2020). High performance fiber-Kevlar the super tough fiber. Journal of Textile Science and Engineering, 10(7), 2–2.

[7] Lustig, S. R., Andzelm, J. W., Wetzel, E. D. (2021). Highly thermostable dynamic structures of polyaramid two-dimensional polymers. Macromolecules, 54(3), 1291–1303.

[8] Chen, X., Zhou, Y. (2016). Technical textiles for ballistic protection. In: Richard Horrocks, A., Anand, S. C. (Eds.). Handbook of technical textiles. 2nd ed. (pp. 169–192). Woodhead Publishing. doi: 10.1016/B978-1-78242-465-9.00006-9.

[9] Cunniff, P. M. (1992). An analysis of the system effects in woven fabrics under ballistic impact. Textile Research Journal, 62(9), 495–509.

[10] Shimek, M. E., Fahrenthold, E. P. (2012). Effects of weave type on the ballistic performance of fabrics. AIAA Journal, 50(11), 2558–2565.

[11] Zhou, Y., Chen, X. (2015). A numerical investigation into the influence of fabric construction on ballistic performance. Composites Part B: Engineering, 76, 209–217.

[12] Zhou, Y., Yao, W., Zhang, Z., Lin, Y., Xiong, Z., Zhao, Y., et al. (2022). Ballistic performance of the structure-modified plain weaves with the improved constraint on yarn mobility: Experimental investigation. Composite Structures, 280, 114913.

[13] Lim, J. S., Lee, B. H., Lee, C. B., Han, I.-S. (2012). Effect of the weaving density of aramid fabrics on their resistance to ballistic impacts. Engineering, 4(12), 944–949.

[14] Wang, Y., Chen, X., Young, R., Kinloch, I. (2016). A numerical and experimental analysis of the influence of crimp on ballistic impact response of woven fabrics. Composite Structures, 140, 44–52.

[15] Xu, L. Z., Ren, W. K., Wang, J. B., Wang, X. D., Gao, G. F. (2023). An experimental investigation into ballistic performance of woven fabrics with single and multiple layers. Textile Research Journal, 93(9–10), 2394–2408.

[16] Das, S., Jagan, S., Shaw, A., Pal, A. (2015). Determination of inter-yarn friction and its effect on ballistic response of para-aramid woven fabric under low velocity impact. Composite Structures, 120, 129–140.

[17] Wang, Y., Chen, X., Young, R., Kinloch, I. (2016). Finite element analysis of effect of inter-yarn friction on ballistic impact response of woven fabrics. Composite Structures, 135, 8–16.

[18] Chu, Y., Chen, X. (2018). Finite element modelling effects of inter-yarn friction on the single-layer high-performance fabrics subject to ballistic impact. Mechanics of Materials, 126, 99–110.

[19] Khodadadi, A., Liaghat, G., Vahid, S., Sabet, A. R., Hadavinia, H. (2019). Ballistic performance of Kevlar fabric impregnated with nanosilica/PEG shear thickening fluid. Composites Part B: Engineering, 162, 643–652.

[20] Wang, X., Zhang, J., Bao, L., Yang, W., Zhou, F., Liu, W. (2020). Enhancement of the ballistic performance of aramid fabric with polyurethane and shear thickening fluid. Materials & Design, 196, 109015.

[21] Xu, Y. J., Zhang, H., Huang, G. Y. (2022). Ballistic performance of B4C/STF/Twaron composite fabric. Composite Structures, 279, 114754.

[22] Mylvaganam, K., Zhang, L. C. (2006). Energy absorption capacity of carbon nanotubes under ballistic impact. Applied Physics Letters, 89(12), 123127.

[23] LaBarre, E. D., Calderon-Colon, X., Morris, M., Tiffany, J., Wetzel, E., Merkle, A., et al. (2015). Effect of a carbon nanotube coating on friction and impact performance of Kevlar. Journal of Materials Science, 50(16), 5431–5442.

[24] Silva, A. O. Da, Weber, R. P., Monteiro, S. N., et al. (2020). Effect of graphene oxide coating on the ballistic performance of aramid fabric. Journal of Materials Research and Technology, 9(2), 2267–2278.

[25] Gloger, M., Stempien, Z. (2022). Experimental Study of Soft ballistic packages with embroidered structures fabricated by using the tailored fiber placement technique. Materials (Basel), 15(12), 4208.

[26] Gloger, M., Stempien, Z., Pinkos, J. (2023). Numerical and experimental investigation of the ballistic performance of hybrid woven and embroidered-based soft armour under ballistic impact. Composite Structures, 322, 117420.

[27] https://www.triaxial.us.

[28] Frontczak-Wasiak, I., Snycerski, M. (2006). Assessment of transversal deformations of multi-axial woven fabrics stretched one-directionally. Fibres & Textiles in Eastern Europe, 14(2), 29–33.

[29] Snycerski, M., Frontczak-Wasiak, I., Balcerzak, M. (2011). Influence of the construction of a four-axial fabric on its properties. Fibres & Textiles in Eastern Europe, 88(5), 40–45.

[30] Czekalski, B., Snycerski, M. (2014). Specific properties of woven multiaxial structures. Fibres & Textiles in Eastern Europe, 22(4), 43–50.

[31] Harle, J. W. S., Leech, C. M., Adeyefa, A., Cork, C. R. (1981). Ballistic impact resistance of multi-layer textile fabrics. University of Manchester INST of Science and Technology (United Kingdom) DEPT of Textile Technology, Manchester.

[32] Giannaros, E., Kotzakolios, A., Sotiriadis, G., Tsantzalis, S., Kostopoulos, V. (2018). On fabric materials response subjected to ballistic impact using meso-scale modeling. Numerical simulation and experimental validation. Composite Structures, 204, 745–754.

[33] Pinkos, J., Stempien, Z. (2020). Numerical and experimental comparative analysis of ballistic performance of packages made of biaxial and triaxial Kevlar 29 fabrics. Autex Research Journal, 20(2), 203–219.

[34] Pinkos, J., Stempien, Z., Smędra, A. (2023). Experimental analysis of ballistic trauma in a human body protected with 30 layer packages made of biaxial and triaxial Kevlar® 29 fabrics. Defence Technology, 21, 73–87.

[35] Karahan, M. (2008). Comparison of ballistic performance and energy absorption capabilities of woven and unidirectional aramid fabrics. Textile Research Journal, 78(8), 718–730.

[36] Chen, X., Zhou, Y., Wells, G. (2014). Numerical and experimental investigations into ballistic performance of hybrid fabric panels. Composites Part B: Engineering, 58, 35–42.

[37] Kedzierski, P., Gieleta, R., Morka, A., Niezgoda, T., Surma, Z. (2016). Experimental study of hybrid soft ballistic structures. Composite Structures, 153, 204–211.

[38] Yang, Y., Ling, T., Liu, Y., Xue, S. (2021). Synergistic effect of hybrid ballistic soft armour panels. Composite Structures, 272, 114211.

[39] Lim, C. T., Shim, V. P. W., Ng, Y. H. (2003). Finite-element modeling of the ballistic impact of fabric armor. International Journal of Impact Engineering, 28(1), 13–31.

[40] Ha-Minh, C., Imad, A., Kanit, T., Boussu, F. (2013). Numerical analysis of a ballistic impact on textile fabric. International Journal of Mechanical Sciences, 69, 32–39.

[41] Zochowski, P., Bajkowski, M., Grygoruk, R., Magier, M., Burian, W., Pyka, D., et al. (2022). Finite element modeling of ballistic inserts containing aramid fabrics under projectile impact conditions – Comparison of methods. Composite Structures, 294, 115752.

[42] Duan, Y., Keefe, M., Bogetti, T. A., Cheeseman, B. A., Powers, B. (2006). A numerical investigation of the influence of friction on energy absorption by a high-strength fabric subjected to ballistic impact. International Journal of Impact Engineering, 32(8), 1299–1312.

[43] Duan, Y., Keefe, M., Bogetti, T. A., Powers, B. (2006). Finite element modeling of transverse impact on a ballistic fabric. International Journal of Mechanical Sciences, 48(1), 33–43.

[44] Wang, Y., Miao, Y., Swenson, D., Cheeseman, B. A., Yen, C. F., LaMattina, B. (2010). Digital element approach for simulating impact and penetration of textiles. International Journal of Impact Engineering, 37(5), 552–560.

[45] Nilakantan, G., Keefe, M., Bogetti, T. A., Gillespie, J. W. (2010). Multiscale modeling of the impact of textile fabrics based on hybrid element analysis. International Journal of Impact Engineering, 37(10), 1056–1071.

[46] Nilakantan, G., Keefe, M., Bogetti, T. A., Adkinson, R., Gillespie, J. W. (2010). On the finite element analysis of woven fabric impact using multiscale modeling techniques. International Journal of Solids and Structures, 47(17), 2300–2315.

[47] Barauskas, R., Abraitiene, A. (2007). Computational analysis of impact of a bullet against the multilayer fabrics in LS-DYNA. International Journal of Impact Engineering, 34(7), 1286–1305.

[48] Yang, E. C., Linforth, S., Ngo, T., Tran, P. (2018). Hybrid-mesh modelling & validation of woven fabric subjected to medium velocity impact. International Journal of Mechanical Sciences, 144, 427–437.

[49] Tripathi, L., Chowdhury, S., Behera, B. K. (2022). Modeling and simulation of impact behavior of 3D woven solid structure for ballistic application. Journal of Industrial Textiles, 51(4), 6065S–6086S.

[50] Barauskas, R., Abraitiene, A. (2013). Multi-resolution finite element models for simulation of the ballistic impact on non-crimped composite fabric packages. Composite Structures, 104, 215–229.

[51] Wang, H., Weerasinghe, D., Mohotti, D., Hazell, P. J., Shim, V. P. W., Shankar, K., et al. (2021). On the impact response of UHMWPE woven fabrics: Experiments and simulations. International Journal of Mechanical Sciences, 204, 106574.

[52] Naik, N. K., Shrirao, P., Reddy, B. C. K. (2006). Ballistic impact behaviour of woven fabric composites: Formulation. International Journal of Impact Engineering, 32(9), 1521–1552.

[53] Lin, J., Li, Y., Liu, S., Fan, H. (2023). Numerical investigation of the high-velocity impact performance of body armor panels. Thin-Walled Structures, 189, 110909.

[54] Shahkarami, A., Vaziri, R. (2007). A continuum shell finite element model for impact simulation of woven fabrics. International Journal of Impact Engineering, 34(1), 104–119.

[55] Tan, V. B. C., Zeng, X. S., Shim, V. P. W. (2008). Characterization and constitutive modeling of aramid fibers at high strain rates. International Journal of Impact Engineering, 35(11), 1303–1313.

[56] Yang, Y., Liu, Y., Xue, S., Sun, X. (2021). Multi-scale finite element modeling of ballistic impact onto woven fabric involving fiber bundles. Composite Structures, 267, 113856.

[57] Kędzierski, P., Morka, A. (2022). A comprehensive approach to the modeling and simulation of ballistic textiles. Composite Structures, 292, 115643.

[58] Dupont. Technical Guide for Kevlar Aramid Fiber. Kevlar_Technical_Guide_0319.pdf, the file uploaded from the www.dupont.com page. 2017.

[59] Buchely, M. F., Maranon, A., Silberschmidt, V. V. (2016). Material model for modeling clay at high strain rates. International Journal of Impact Engineering, 90, 1–11.

[60] Hernandez, C., Buchely, M. F., Maranon, A. (2015). Dynamic characterization of Roma Plastilina No. 1 from Drop Test and inverse analysis. International Journal of Mechanical Sciences, 100, 158–168.

[61] Zhang, T. G., Ivancik, J., Mrozek, R. A., Satapathy, S. S. (2017). Material characterization of ballistic Roma Plastilina No. 1 clay. 30th International Symposium on Ballistics. Sep 11–15; Long Beach, CA. doi: 10.12783/ballistics2017/17041.

[62] Martínez, M. A., Navarro, C., Cortés, R., Rodríguez, J., Sanchez-Galvez, N. (1993). Friction and wear behaviour of Kevlar fabrics. Journal of Materials Science, 28(5), 1305–1311.

[63] Rao, M. P., Duan, Y., Keefe, M., Powers, B. M., Bogetti, T. A. (2009). Modeling the effects of yarn material properties and friction on the ballistic impact of a plain-weave fabric. Composite Structures, 89(4), 556–566.

[64] Zochowski, P., Bajkowski, M., Grygoruk, R., Magier, M., Burian, W., Pyka, D., et al. (2021). Ballistic impact resistance of bulletproof vest inserts containing printed titanium structures. Metals (Basel), 11(2), 1–23.